Metrol. Meas. Syst., Vol. 26 (2019) No. 2, pp. 297–308.

PAN POLSKA AKADEMIA NAUK

METROLOGY AND MEASUREMENT SYSTEMS

Index 330930, ISSN 0860-8229

www.metrology.pg.gda.pl

M&MS

MORPHOLOGICAL DISCRIMINATION OF GRANULAR MATERIALS BY MEASUREMENT OF PIXEL INTENSITY DISTRIBUTION (PID)

Artur Wójcik[1)], Piotr Kościelniak[2)], Marcin Mazur[2)], Thomas G. Mathia[3)]

1) *University of Agriculture in Krakow, Faculty of Production and Power Engineering, Balicka 120, 30-149, Cracow, Poland* (✉ *artur.wojcik@urk.edu.pl*, +48 12 662 4678)

2) *Jagiellonian University, Faculty of Mathematics and Computer Science, Łojasiewicza 6, 30-348 Cracow, Poland* (*piotr.koscielniak@uj.edu.pl*, *marcin.mazur@uj.edu.pl*)

3) *Ecole Centrale de Lyon, Laboratoire de Tribologie et Dynamique des Systèmes LTDS, CNRS, France* (*thomas.mathia@ec-lyon.fr*)

Abstract

The paper provides statistical analysis of the photographs of four various granular materials (peas, pellets, triticale, wood chips). For analysis, the (parametric) ANOVA and the (nonparametric) Kruskal-Wallis tests were applied. Additionally, the (parametric) two-sample t-test and (non-parametric) Wilcoxon Rank-Sum Test for pairwise comparisons were performed. In each case, the Bonferroni correction was used. The analysis shows a statistical evidence of the presence of differences between the respective average discrete *pixel intensity distributions* (PID), induced by the histograms in each group of photos, which cannot be explained only by the existing differences among single granules of different materials. The proposed approach may contribute to the development of a fast inspection method for comparison and discrimination of granular materials differing from the reference material, in the production process.

Keywords: granular material, digital image analysis, pixel intensity distribution, discrimination process control.

1. Introduction

Right after water, granular materials are the most commonly used materials in industry. They are processed in virtually every area of economy, *i.e.*, agriculture (seeds, mineral fertilizers, grains, animal feed), food (flour, comminuted fruit and vegetables, cereal), pharmaceutics and cosmetics (reinforcing materials, powders), construction (aggregates, cement, sand), energy (slag, coal, comminuted biomass).

One can easily imagine that inter-granular organization depends on morphology of granular materials influencing the mobility and therefore their associations and arrangements.

In the fields of agriculture, geology and biology, morphology can be understood as the study of the shapes and distribution of particles (grains). A two-dimensional digital image is a specific way of illustrating this morphology.

Article history: received on Nov. 17, 2018; accepted on Dec. 29, 2018; available online on Jun. 28, 2019; DOI: 10.24425/mms.2019.128357.

Consequently, the measurements of granular descriptors, such as nature, size, morphology *etc*., are fundamental problems in grain mass production and/or transformation, transportation and packaging.

The basic problem in metrology is the determination of precision, measurement accuracy and the associated true value. According to [1], accuracy of measurement is "closeness of the agreement between the result of a measurement and a true value", which is related to the occurrence of random and systematic errors [2, 3]. It should be noted that in many aspects of measurement of granular materials, we do not know the true value which we can refer measurement results to. Therefore, we cannot talk about the accuracy of measurement. That is why measurements of this type of materials rise many metrological and mathematical problems.

There is a great number of technological situations where robustness (*i.e.*, correctness) of methodology is the most important aspect of measurements. That is the main motivation of the research described below. Therefore, this paper describes the process of verifying the robustness of "test cases" in a test process looking for compromise between economically tolerant and metrologically simple and acceptable methodology.

Traditional metrology of granular assemblies (Fig. 1) is too time-consuming and too expensive. Therefore, a new, simple, fast and cheap methodology has been offered and validated in the present paper.

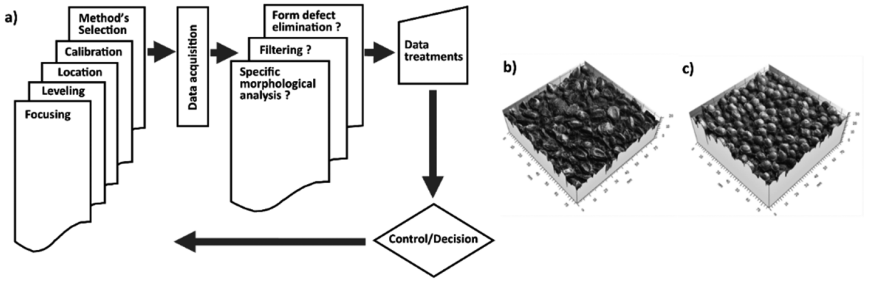

Fig. 1. Complex sequences a) of data treatments necessary to identify the differences in particle morphology thanks to a 3D optical scanner. (The sequence of fringe images are projected onto the material by an LCD projector and then the distances of every point are calculated to obtain the surface geometry). Using white LED light technology, selected pictures of maize b) and of pea c) clearly show the differences in morphologies.

Computer image analysis and vision systems, an integral part of which is *Digital Image Analysis* (DIA), are used in many areas, such as medicine, security, material quality control, *etc.* The usual procedure of DIA can be divided into the following steps: image acquisition, image processing, image analysis, recognition and interpretation (Fig. 2).

The understanding of the behaviour and physical properties of granular material is of fundamental importance to the optimization of such processes as transport and storage, dispensing, grinding, mixing, agglomeration. This knowledge provides also a sound basis for the design or improvement of machinery and equipment used in these processes. Regardless of the type of granular materials, they exhibit common physical properties such as porosity, bulk density, particle-size distribution, shape (geometric dimensions), static and kinetic friction, and the angle of repose [4–9].

The analysis of issues concerning DIA in a context of the physical characteristics of granular materials focuses on three main areas: the analysis of single grains (*e.g.*, the size of particles) [10–14], the analysis of the bulk as a whole (*e.g.*, bulk density, porosity) [15–17], and the analysis of processes, *e.g.*, in a context of their monitoring and control [18–22].

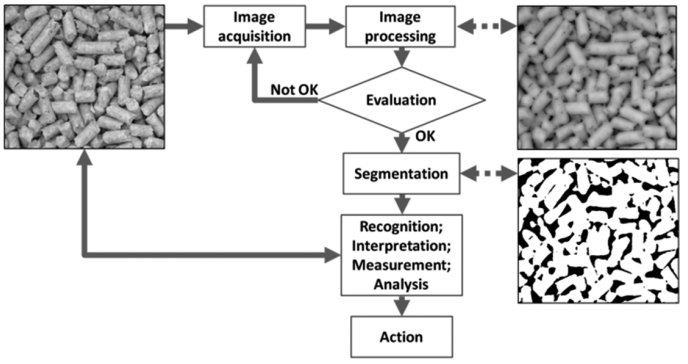

Fig. 2. A flowchart (traditional steps) of Digital Image Analysis applied to plant granular materials.

Classical methods for the measurement of physical properties of granular materials are usually time-consuming, which often turns against them in dynamic production processes with a high degree of automation, and when it is necessary to process large amounts of information in real time. Therefore, DIA, which has become a pretty viable and efficient method for evaluation of a variety of features and properties exhibited by the tested objects, is increasingly in use.

In this publication, the authors have proposed a slightly extended approach to the image analysis, in which a photograph is treated as a carrier of certain statistical information.

Let us assume that we take a photograph of granular material, in which the grains are not identical (*e.g.*, cereal grains), then mix the grains and take another photo. As a consequence, we obtain two different pictures (different number of seeds, different orientation, *etc*.) showing the same granular material. How can we confirm that both photos represent the same material? It turns out that the approach presented in Fig. 2, where we are looking for some specific feature, *e.g.*, grain size or shape, may be inappropriate.

The analysis becomes more complicated if we want to indicate differences between the same material if one of them has, for example, a different moisture or packing degree. It is important because grainy materials are processed in automated continuous processes. Therefore, it seems to be crucial to develop and refine the initial and rapid quality control processes of this material.

The pictures of granular material containing a lot of objects of a similar nature, structure, seem to be a perfect subject of such an analysis. In particular, our aim is to explore some subtle information that is "hidden" in photographs "taken from above", *i.e*. showing only surface layers of prescribed portions of few granular materials, which can be interpreted as confirmation of the existence of some "global" (whole picture) differences related to their (possibly spatial) structure that cannot be explained by the existing "local" (single grain) differences, *e.g.*, in pixel intensity, among single granules of materials under consideration.

2. Selected materials

In our study, we use four granular materials that are typical in agriculture, *i.e*. peas, pellets, triticale and wood chips (Fig. 3). The two of them (peas and triticale) represent grains used in food processing, the other two (pellets and wood chips) – biomass used for energy purposes.

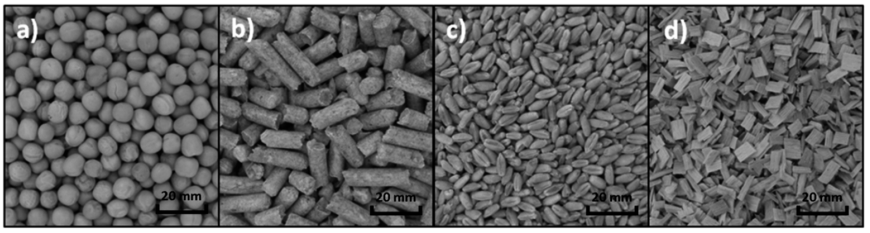

Fig. 3. Photos of examined organic materials: a) peas; b) pellets; c) triticale; d) wood chips.

3. Measuring procedure and robustness validation

The images of granular materials were acquired in a specially prepared station consisting of a tripod, a Nikon D800 digital camera, a shadow-less tent, lighting. The images of the tested materials were captured in the same acquisition conditions. Subsequently, they were analysed with the use of software Aphelion Dev, which is part of Aphelion Imaging Software Suite [29].

3.1. Opening data processing

The same conditions were retained when preparing the material for image acquisition. The tested material was poured freely from the same height into a flat container. Excess material was scraped. A sample so prepared was placed in the shadow-less tent. For each material, 10 images were collected. Then, each image was properly trimmed so that it contained the same amount of pixels which is the smallest controllable element of an image presented in the picture.

Then, for the images, histograms were generated. The histogram generation from part of a greyscale image composed of 25 pixels is shown in Fig. 4. The four pixel intensities (Fig. 4a) (including black and white) of this image are represented by the four vertical lines of the associated histogram (Fig. 4b). Here, values on the horizontal axis are in a range from 0 to 255, which is consistent with a standard numeric representation of the greyscale. The value "0" corresponds to the black colour, while the value "255" corresponds to the white colour.

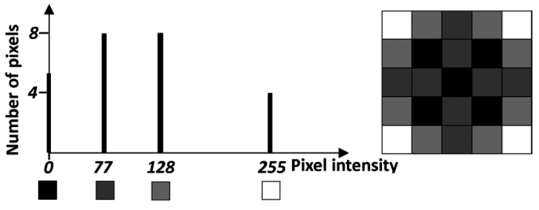

Fig. 4. The principle of pixel histogram generation versus pixel intensity (greyscale): a) a histogram; b) a decomposed image in 25 pixels.

The same principle applies to a colour image, in this case, however, we deal with three histograms corresponding respectively to the intensity of components of three primary colours, *i.e.*, red (R), green (G), blue (B). In our case, we analysed images that were converted from a colour image into a greyscale image according to (1). Then, histograms were created for the so prepared images.

$$Pixel\ intensity = \frac{Intensity(R) + Intensity(G) + Intensity(B)}{3}. \tag{1}$$

In general, one can indicate here that the differences between pictures might be caused by different colour intensity of the materials under consideration. Taking into account that all the photographs were taken in the same conditions, we claim that further processing of our data, such as some kind of intensity standardization that is used in analysis of MRI images [23, 24], seems to be unnecessary.

As it was previously indicated, in the paper we investigate the problem of exploration of some information that is "hidden" in photographs showing only surface layers of prescribed portions of given granular materials. This can be used to obtain a statistical confirmation of the existence of some differences related to their (possibly spatial) structure.

Speaking formally, assume that we have m groups of photos, each of them representing some established tested material. By n_j we denote the cardinality of the j-th group, *i.e.*, the number of photos of the j-th material, where $j \in \{1, \ldots, m\}$. For $k \in \{1, \ldots, n_j\}$, we consider the histogram (in some monochromatic scale) $h_{j,k}$ of the k-th photo in the j-th group, *i.e.*, the numbers (denoted by $y_{j,k,i}$) of pixels with color intensity i for $i \in \{0, \ldots, 255\}$. Let $S_{j,k} = \sum_{i=0}^{255} y_{j,k,i}$ be the sum of pixels in the k-th photo of the j-th tested material and let define $p_{j,k,i} = y_{j,k,i}/S_{j,k}$. Let us notice that then $d_{j,k} = (p_{j,k,0}, \ldots, p_{j,k,255})$ can be considered as a discrete distribution of *pixel intensity* (PID) of the k-th photo in the j-th group (Fig. 5).

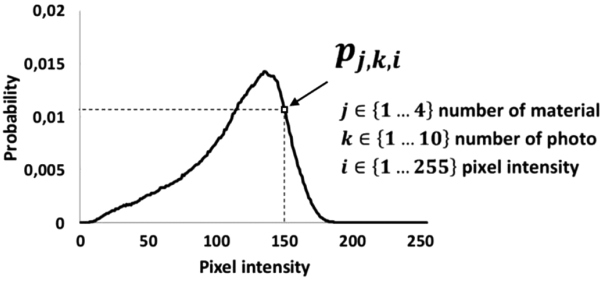

Fig. 5. An illustration of a smoothed PID.

The aim of this section is, roughly speaking, to propose a method, basing on some advanced techniques of inferential statistics, which enables to verify the differences between the groups of distributions $G_j = \left\{d_{j,k}\right\}_{k=1}^{n_j}$ for $j \in \{1, \ldots, m\}$.

3.2. Methodology

Referring to the above introduced notation and assumptions, in this subsection we present the method that enables to test a hypothesis that the average distributions, which can be calculated in a usual way (see below) for each group Gj, where $j \in \{1, \ldots, m\}$, are not statistically different. To do this, we propose some methods that are based on known hypothesis testing techniques involving both parametric and nonparametric approaches, combined with suitable adjustments usually required for multiple testing problems, *i.e.* Bonferroni correction. In particular, this method controls the total probability of type I error, to avoid the effect of too frequent rejection in the case of many hypotheses tested together.

In particular, let us notice at first that it is possible to look separately for every i-th "coordinate" of our data set, where $i \in \{0, \ldots, 255\}$, to yield in each case (new) groups of "one-dimensional"

data that look as follows:

$$\begin{aligned} G_1^i &= \{p_{1,1,i},\ \ldots,\ p_{1,n_1,i}\}, \\ G_2^i &= \{p_{2,1,i},\ \ldots,\ p_{2,n_2,i}\}, \\ &\vdots \\ G_m^i &= \{p_{m,1,i},\ \ldots,\ p_{m,n_m,i}\}. \end{aligned} \tag{2}$$

Hence, for each i we can test the null hypothesis H_0^i, which says that probability of finding a pixel of intensity i in a given photo is (on average) the same for each tested materials. Let pva_i and pvk_i denote p-values associated with the hypothesis H_0^i, using the (parametric) ANOVA [25] and (nonparametric) Kruskal-Wallis [26, 27] tests, respectively. Then, to conclude our procedure, it is enough to test a "complete" null hypothesis H_0 that is the conjunction of all null hypotheses H_0^i for $i \in \{0, \ldots, 255\}$, which can be interpreted as a statistical confirmation of the equality of all average distributions (this procedure is also known as the multiple comparisons or the multiple testing problem). To achieve this, we can apply a so called Bonferroni correction [28] in order to calculate respective p-values related to both above mentioned approaches, which are:

$$pva = \min\{256 \cdot pva_0,\ \ldots,\ 256 \cdot pva_{255},\ 1\}, \tag{3}$$

in the case of the ANOVA test, and

$$pvk = \min\{256 \cdot pvk_0,\ \ldots,\ 256 \cdot pvk_{255},\ 1\}, \tag{4}$$

in the case of the Kruskal-Wallis test, respectively. Finally, it should be emphasized here that the smaller values of pva and pvk (with the usual threshold at 0.01, 0.05 or 0.1), the greater statistical confidence that differences between (the average distributions in) the groups G_j for $j \in \{1, \ldots, m\}$ really exist.

In the further analysis (pairwise comparisons), the situation is similar. For a given pair of materials, let pvt_i and pvw_i denote p-values associated with the hypotheses H_0^i, using the (parametric) t-test [25] and (nonparametric) Wilcoxon [26, 27] test, respectively. Similarly, we consider the null hypothesis H_0 that consists of all null hypotheses H_0^i for $i \in \{0, \ldots, 255\}$ and we use the Bonferroni correction. Finally, we obtain:

$$pvt = \min\{256 \cdot 6 \cdot pvt_0,\ \ldots,\ 256 \cdot 6 \cdot pvt_{255},\ 1\}, \tag{5}$$

in the case of the t-test, and

$$pvw = \min\{256 \cdot 6 \cdot pvw_0,\ \ldots,\ 256 \cdot 6 \cdot pvw_{255},\ 1\}, \tag{6}$$

in the case of the Wilcoxon test, respectively.

3.3. Principal results

It should be reminded that in the process of data treatment for each of 4 different granular materials: peas, triticale, wood chips and pellets, we had 10 photographs of their various prescribed portions. The analysis was carried out for three image sizes (1233×1200, 733×700, 233×200 pixels) and for photographs containing a single grain. The authors suspect that the proposed method of discrimination, by means of a statistical analysis, will be effective when there is a sufficiently large number of grains and crevices, further called pores, in the picture. That was

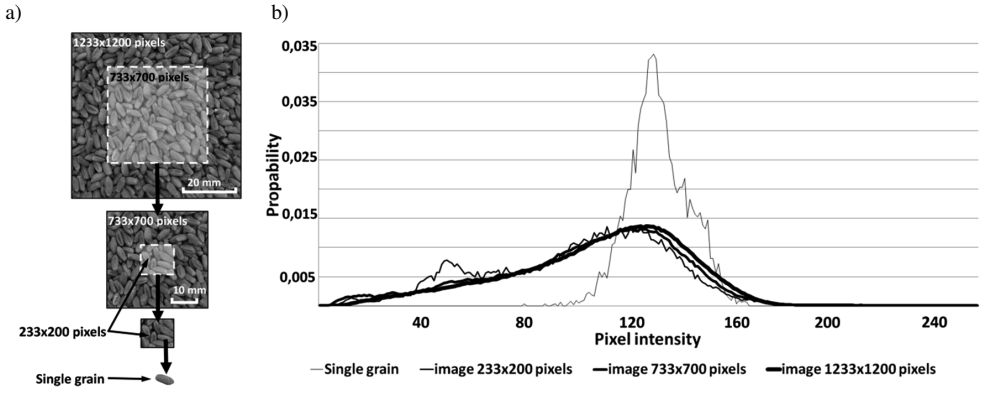

Fig. 6. a) The procedure of "cutting out" a "central" part; b) an example of a change in the form of distribution for a particular "photo size", with respect to triticale.

experimentally confirmed. The idea of "cutting out" subsequent sizes of a photo is shown in Fig. 6a, whereas Fig. 6b shows a change in distribution of pixel intensity for each image size, on an example of triticale.

A PID was assigned to each of 10 photographs of each material at different "cutting out" size shown in Figures 7 to 10. From the initial interpretation of distributions obtained in that way, it can be noticed that with the reduction of the analysis area in individual photos, the variability of distributions increases. Therefore, the authors conclude that the size of a photo (the amount of grains in a picture) can have a significant impact on the reliability of the obtained results.

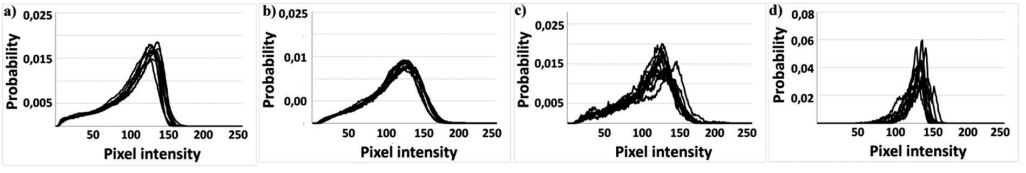

Fig. 7. PID graphs for peas for particular photo sizes: a) 1233 × 1200 pixels; b) 733 × 700 pixels; c) 233 × 200 pixels; d) a single grain.

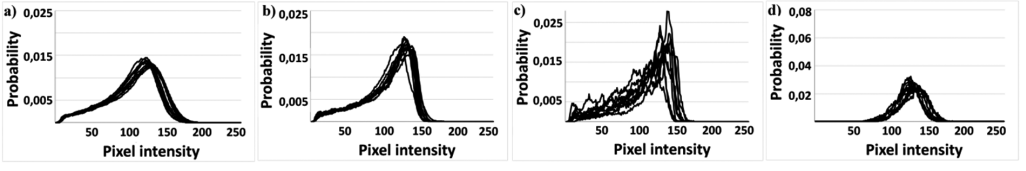

Fig. 8. PID graphs for pellets for particular photo sizes: a) 1233 × 1200 pixels; b) 733 × 700 pixels; c) 233 × 200 pixels; d) a single grain.

According to the procedure described in Subsection 3.2 and the procedure of "cutting out" (Fig. 5), *p*-values were determined. However, the analysis was carried out in two stages. In the first stage, for each image size, four materials were examined together with the view of checking whether there were statistical differences between these materials. The results are presented in Fig. 11.

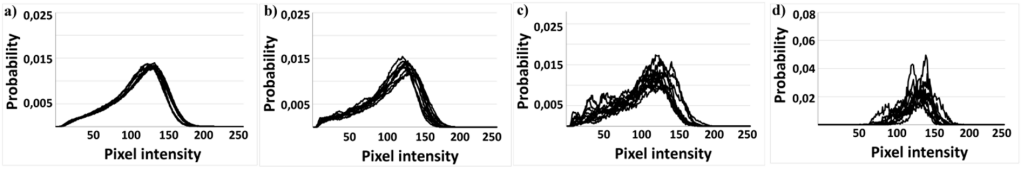

Fig. 9. PID graphs for triticale for particular photo sizes: a) 1233 × 1200 pixels; b) 733 × 700 pixels; c) 233 × 200 pixels; d) a single grain.

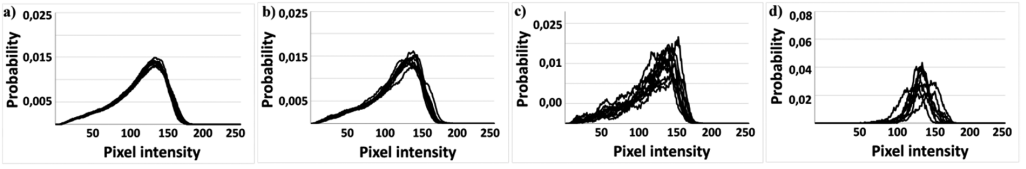

Fig. 10. PID graphs for woodchips for particular photo sizes: a) 1233×1200 pixels; b) 733×700 pixels; c) 233×200 pixels; d) a single grain.

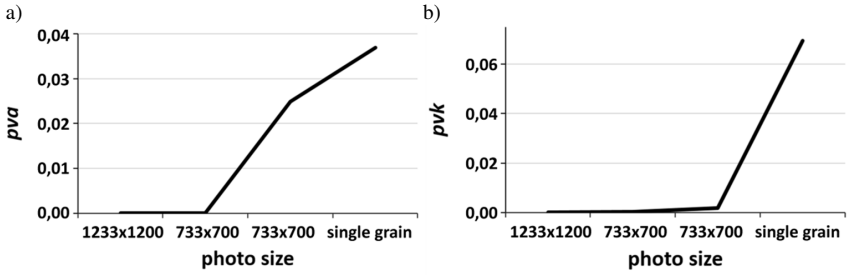

Fig. 11. Graphs of *pva* and *pvk* for a group of four materials versus image size.

The second stage of the analysis consisted in comparing the materials in pairs. Six combinations were obtained for each image size. The results are presented in Figs. 12 and 13.

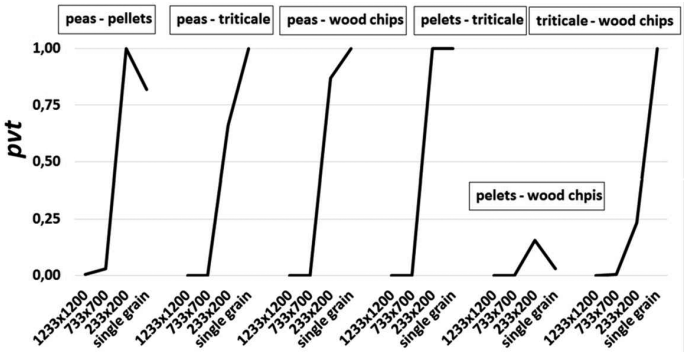

Fig. 12. The values of *pvt* for comparison of each pair of materials, depending on the image size.

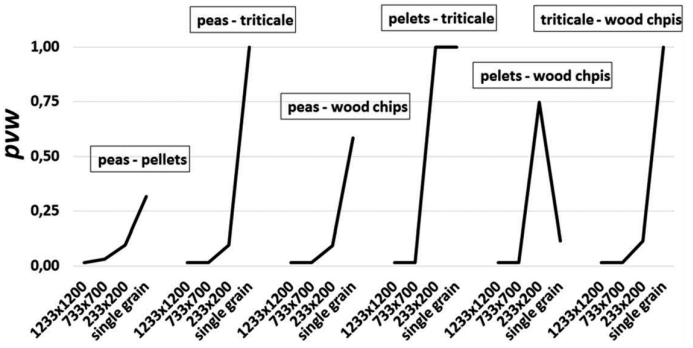

Fig. 13. The values of *pvw* for comparison of each pair of materials, depending on the image size.

4. Preliminary conclusions

In the global analysis of robustness, *i.e.* testing all materials at once (Fig. 11), significant differences between the analysed materials (*pva*, *pvk* less than 0.05 for image sizes 1233×1200, 733×700 and 233×200 pixels) were observed. It has to be noticed that *pva* and *pvk* grow as the analysis area decreases. In the case of the "single grain" analysis, using the Kruskal-Wallis test, the lack of significant differences in the PID between photographs of individual materials (grains) can be stated. In summary, it can be therefore concluded that along with the reduction of the analysis area, the statistical differences between photos decrease.

When compared in pairs (Figs. 12 and 13), a similar and more pronounced result was obtained. For each of the two established materials, the photos differed statistically for the large analysis area, whereas they were not statistically different for the smaller area of analysis. Accordingly, evolutions of the *pvw* and *pvt* parameters are commonly monotonic. The observed exceptions may result from the statistical nature of analyses, for example, the potentially unfulfilled (difficult to verify) assumptions (see more details below) or a low test power resulting from a relatively reduced quantity of samples.

Let us recall that all applied methods of our analysis, *i.e.* the (parametric) ANOVA and the t-test as well as the (non-parametric) Kruskal-Wallis test and the Wilcoxon rank-sum test, led to similar conclusions. It has to be emphasized that the assumptions underlying the parametric methods, *i.e.* normally distributed samples (normality) and equal variances (homoscedasticity) for each of the groups (in the case of ANOVA), which are not required by the Kruskal-Wallis or Wilcoxon procedure, have not been verified since our dataset was not sufficiently large to apply any limit approximation. Thus, regardless of the fact that nonparametric tests are not as powerful as parametric ones, the results obtained from the nonparametric procedure seem to provide, at least from a formal point of view, a more reliable basis for any conclusion.

The specific type of objects visible in the pictures of granular materials, *i.e.* a lot of tiny elements of a varying shape with darker fields (pores) between them, requires a slightly different approach to be taken to analysis. For example, confirmation of whether or not two different pictures of a given material represent the same material does not have to be so obvious to automatic vision systems. Most importantly, the obtained results lead to a conclusion that the proposed statistical approach, although it still requires further improvements, can provide a basis for the development of a quick inspection method for detecting differences between photographed granular materials used in various processes.

The PID and consequently the determined $p-$value (*pva, pvk, pvt, pvw* – depending on the test performed) are influenced by many factors related to the physical properties of the examined objects (grains). Generally, these values depend on the PID located in the grain (objects) and the pore areas (Fig. 14a).

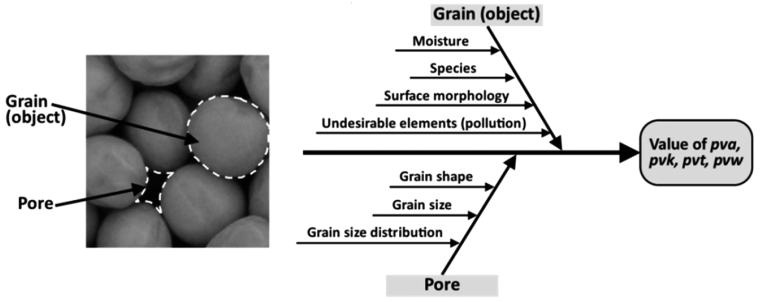

Fig. 14. The factors affecting the pixel intensity distribution: a) part of the analysed image; b) main factors.

The PID of grains can depend on moisture, species, impurities, surface morphology. However, the PID located in the pore area is a derivative of physical properties such as shape and size of grains.

Therefore, any stabilized process, *e.g*. dosing of a certain granular material, can be disturbed by changing one of the factors listed in Fig. 14b. This will change the PID of the entire image. By testing (comparing) the distributions obtained according to the procedure of Subsection 3.2 with the reference distributions for a given granular material, similarities or differences can be found in relation to the reference material (Fig. 15).

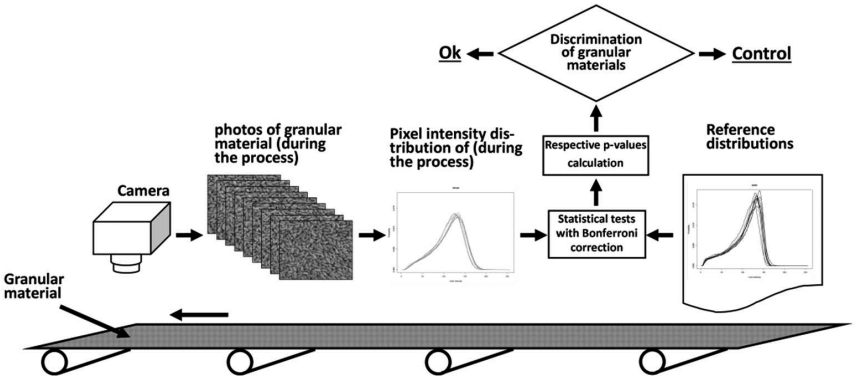

Fig. 15. A schematic of "on line" system application to the discrimination of plant granular materials.

5. Software facilities

All computations were performed by applying suitable procedures implemented by the authors in R programming language (http://www.r-project.org), offering an open-source platform for various methods of data analysis, including statistical inference techniques and data mining tools. The source codes can be downloaded by the reader from our website (*http://www2.im.uj.edu.pl/PiotrKoscielniak/granular_code.R*) under the terms of the GNU General Public License.

Acknowledgements

This research was supported by the Ministry of Science and Higher Education of the Republic of Poland.

Nomenclature, symbols and abbreviations

ANOVA – Analysis of Variance
DIA – Digital Image Analysis
PID – Pixel Intensity Distribution
$y_{j,k,i}$ – the number of pixels with pixel intensity i for k-th photo in j-th group
$S_{j,k}$ – sum of pixels for k-th photo in j-th group
$d_{j,k}$ – PID for k-th photo in j-th group
H_0 – null hypothesis
pva, pvk, pvt, pvw – respective p-values, *i.e.*, the smallest significant levels at which H_0 is rejected, for ANOVA, Kruskal-Wallis test, t-test and Wilcoxon test.

References

[1] BIPM, IEC, IFCC, ISO, IUPAC, IUPAP, OIML: *Guide to the Expression of Uncertainty in Measurement*. International Organization for Standardization, Geneva. First Edition 1993, corrected and reprinted 1995.

[2] Wójcik, A., Niemczewska-Wójcik, M., Sładek, J. (2017). Assessment of free-form surfaces' reconstruction accuracy. *Metrol. Meas. Syst.*, 24(2), 303–312.

[3] Niemczewska-Wójcik, M., Sładek, J., Tabaka, T., Wójcik, A. (2014). Product quality assessment – measurement and analysis of surface topography. *Metrol. Meas. Syst.*, 21(2), 271–280.

[4] Mathia, T.G., Pawlus P., Wieczorowski M. (2011). Recent trends in surface metrology. *Wear*, 271, 3–4, 494–508.

[5] Królczyk, J.B. (2016). Metrological changes in the surface morphology of cereal grains in the mixing process. *Int. Agrophys.*, 30, 193–202.

[6] Markowski, M., Żuk-Gołaszewska, K., Kwiatkowskia, D. (2013). Influence of variety on selected physical and mechanical properties of wheat. *Industrial Crops and Products*, 47, 113– 117.

[7] Wójcik, A., Frączek, J., Wota, A.W. (2019). The methodical aspects of the friction modeling of plant granular materials. *Powder Technology*, 344, 504–513.

[8] Wójcik, A., Klapa, P., Mitka, B., Sładek, J. (2018). The use of the photogrammetric method for measurement of the repose angle of granular materials. *Measurement*, 115, 19–26.

[9] Wójcik, A., Frączek, J. (2017). The influence of the repose angle and porosity of granular plant materials on the angle of internal friction and cohesion. *Tribologia*, 5, 117–123.

[10] Rezaei, H., Jim Lim, C., Lau, A., Sokhansanj, S. (2016). Size, Shape and Flow Characterization of Ground Wood Chip and Ground Wood Pellet Particles. textitPowder Technology.

[11] Hartmann, H., Böhm, T., Jensenb, P.D., Temmerman, M., Rabierc, F., Golserd, M. (2006). Methods for size classication of wood chips. *Biomass and Bioenergy*, 30, 944–953.

[12] Kristensen, E.F., Kofman, P.D. (2000). Pressure resistance to air flow during ventilation of different types of wood fuel chip. *Biomass and Bioenergy*, 18, 175–180.

[13] Mattsson, J.E. (1990). Basic handling characteristics of wood fuel: angle of repose, friction against surfaces and tendency to bridge building for different assortments. *Scandinavian Journal of Forest Research*, 5, 583–597.

[14] Jensen, P.D., Mattsson, J.E., Kofman, P.D., Klausner, A. (2004). Tendency of wood fuels from whole trees, logging residues and roundwood to bridge over openings. *Biomass and Bioenergy*, 26, 107–113.

[15] Nabawy, B.S. (2014). Estimating porosity and permeability using Digital Image Analysis (DIA) technique for highly porous sandstones. textitArab J. Geosci.

[16] Andrä, H., Combaret, N., Dvorkin, J., Glatt, E., Han, J., Kabel, M., Keehm, Y., Krzikalla, F., Lee, M., Madonna, C, Marsh, M., Mukerji, T., Saenger, E.H., Sain, R., Saxena, N., Ricker, S., Wiegmann, A., Zhan, X. (2013). Digital rockphysicsbenchmarks-Part I: Imagingandsegmentation. *Computers & Geosciences*, 50, 25–32.

[17] Wójcik, A., Przybyla, W., Francik, S., and Knapczyk, A. (2018). The Research into Determination of the Particle-Size Distribution of Granular Materials by Digital Image Analysis. Mudryk, K., Werle, S. eds., *Renewable energy sources: engineering, technology, innovation: ICORES 2017*. Springer International Publishing AG, 623–630.

[18] Ahmed, F., Hawlader, A.Al-M., Hossain Bari, A.S.M., Hossain, E., Kwanb, P. (2012). Classification of crops and weeds from digital images. *A support vector machine approach. Crop Protection*, 40, 98–104.

[19] Roscher, R., Herzog, K., Kunkel, A., Kicherer, A., Töpfer, R., Förstner, W. (2014). Automated image analysis framework for high-throughput determination of grapevine berry sizes using conditional random fields. *Computers and Electronics in Agriculture*, 100, 148–158.

[20] Wang, Q., Wanga, H., Xie, L., Zhang, Q. (2012). Outdoor color rating of sweet cherries using computer vision. *Computers and Electronics in Agriculture*, 87, 113–120.

[21] Yadav, B.K., Jindal, V.K. (2001). Monitoring milling quality of rice by image analysis. *Computers and Electronics in Agriculture*, 33, 19–33.

[22] Liu, W., Tao, Y., Siebenmorgen, T.J., Chen, H. (1998). Digital Image Analysis Method for Rapid Measurement of Rice Degree of Milling. *Cereal Chem.*, 75, 380–385.

[23] Nyul, L.G., Udupa, J.K. (1999). On Standardizing the MR Image Intensity Scale. *Magnetic Resonance in Medicine*, 42, 1072–1081.

[24] Khoo, S.W., Karuppanan, S., Tan, C.S. (2016). *A review of surface deformation and strain measurement using two-dimensional digital image correlation*. 23(3), 461–480.

[25] Hocking, R.R. (2003). *Methods and Applications of Linear Models: Regression and the Analysis of Variance, Wiley Series in Probability and Statistics*. John Wiley & Sons, New York.

[26] Kruskal, W.H., Wallis, W.A. (1952). Use of ranks in one-criterion variance analysis. *Journal of the American Statistical Association*, 47, 583–621.

[27] Hollander, M., Wolfe, D.A. (1973). *Nonparametric Statistical Methods*. John Wiley & Sons, New York.

[28] Bretz, F., Hothorn, T., Westfall, P. (2010). *Multiple Comparisons Using R*. CRC Press.

[29] Aphelion Imaging Software Suite, *http://www.adcis.net/en/Products/Aphelion-Imaging-Software-Suite.html*.